

## Current status of GaN crystal growth by sublimation sandwich technique

P. G. Baranov<sup>1</sup>, E. N. Mokhov<sup>1</sup>, A. O. Ostroumov<sup>1</sup>, M. G. Ramm<sup>1</sup>, M. S. Ramm<sup>1</sup>, V. V. Ratnikov<sup>1</sup>, A. D. Roenkov<sup>1</sup>, Yu. A. Vodakov<sup>1</sup>, A. A. Wolfson<sup>1</sup>, G. V. Saparin<sup>2</sup>, S. Yu. Karpov<sup>3</sup>, D. V. Zimina<sup>3</sup>, Yu. N. Makarov<sup>4</sup> and Holger Juergensen<sup>5</sup>

<sup>1</sup>*Ioffe Physical-Technical Institute,*

<sup>2</sup>*Moscow State Lomonosov University,*

<sup>3</sup>*Soft-Impact Ltd (St.Petersburg, Russia),*

<sup>4</sup>*Lehrstuhl für Strömungsmechanik, University of Erlangen-Nürnberg,*

<sup>5</sup>*AIXTRON AG,*

(Received Monday, August 31, 1998; accepted Monday, November 2, 1998)

The current status of GaN crystal growth using the Sublimation Sandwich Technique is discussed in the paper. We use modeling to analyze gas dynamics in the reactor and the supply of the main gaseous species into the growth cell under growth conditions used in experiments. Important features of growth process — non-equilibrium cracking of ammonia, partial sticking of ammonia at the growing surface and kinetic limitation of GaN thermal decomposition — are taken into account in the model. Growth is carried out on sapphire and 6H-SiC substrates in ammonia atmosphere using a Ga/GaN mixture as the group-III element source. Single crystals of GaN of size 15×15 mm and up to 0.5 mm thick are normally grown with the optimized growth rates of 0.25-0.35 mm/h. The GaN crystals are characterized by photoluminescence, by the Color Cathodoluminescence Scanning Electron Microscopy technique, by differential double-crystal and triple-crystal X-ray diffractometry, and by electron paramagnetic resonance. Mechanisms of sublimation growth of GaN and physical limitations of the growth process are discussed.

### 1 Introduction

Homoeopitaxy on GaN substrates is one of the successful ways of fabricating device-quality nitride-based heterostructures. To get such substrates, bulk GaN crystals of an appropriate size are necessary. Nowadays three techniques can be regarded as promising to obtain GaN bulk crystals – High Pressure Crystal Growth [1], Chloride Hydride Vapor Phase Epitaxy (especially in combination with lateral regrowth) [2], and Sublimation Sandwich Technique [3]. The latter has been initially developed for growth of high-quality SiC crystals and then applied to group-III nitrides, first of all, to GaN [4]. Recently the sublimation technique also succeeded in growth of large size AlN crystals [5].

The sublimation technique is one of the traditional ways to grow bulk AlN crystals [6]. This is possible due to congruent evaporation of this material at high temperatures providing nearly stoichiometric composition of the vapor phase. The pressure of the main species (Al and N<sub>2</sub>) over a AlN surface reaches ~1 atm only at

2260°C. That is the reason why the temperature range of 1950-2250°C is normally used for sublimation growth of AlN. As a result crystals up to 1 mm thick with the size of 10×10 mm can be obtained by this technique.

In contrast to the case of AlN the nitrogen pressure over GaN under practical growth conditions (temperatures ~1000°C) lies between ~10 and ~100 bars. Vaporization of GaN at high temperatures is congruent only under Langmuir conditions (free evaporation in vacuum) [7]. At higher pressures (i.e. closer to equilibrium conditions) evaporation of GaN becomes non-congruent and is accompanied by liquid Ga accumulation on the surface. As a result molecular nitrogen dominates in the vapor phase. However, because of extremely low chemical reactivity of N<sub>2</sub> on GaN surfaces, growth of GaN under these conditions does not occur. Hence external flow of nitrogen-containing reactive species is required to initiate the growth process. The best choice of such species in all respects is ammonia.

Apparently first free-standing GaN crystals of considerable size have been obtained by growth from the vapor phase in [8]. In this work synthesized GaN powder was heated in dry  $\text{NH}_3$  flow at 1150-1200°C for 24 hours. This resulted in growth of GaN crystals of a needle shape and of size  $5 \times 1$  mm. The author of [8] concluded that growth of GaN occurs via sintering although the contribution of the physical vapor transport seems to be also important under these conditions.

Growth of GaN using ammonia passing over liquid gallium was carried out at 1000-1150°C in an open or partly closed quartz ampoule [9]. In the latter case  $\text{NH}_3$  was supplied to a boat with liquid Ga through a small orifice of 1 mm in diameter that provided diffusion limited growth conditions. GaN was deposited on the walls of the ampoule in the form of whiskers, needles, platelets etc. It was concluded in Ref. [9] that the GaN crystals had been grown from the vapor phase containing atomic gallium and ammonia. In addition it was also shown that raising the growth temperature made it possible to increase the size of grown GaN crystals [10].

Detailed study of mechanisms of GaN crystallization due to reaction of Ga vapor with ammonia was carried out in Ref. [11]. A wide range of temperature, 825-1010°C, and  $\text{NH}_3$  pressure, 0.3-2.5 mbar were used for growth, and prismatic GaN crystals appeared in the reactor. The largest crystals (up to 2.5 mm long) were formed on SiC or GaN seeds. These crystals had the electron concentration  $n \sim 10^{19} \text{ cm}^{-3}$  with a mobility of  $100 \text{ cm}^2/\text{V}\cdot\text{s}$ .

Therefore attempts to growth free-standing GaN crystals in Ga- $\text{NH}_3$  system without seed or substrate were not successful. In the best case, needle or platelet crystals were obtained but their lateral size was very far from desirable. In Refs. [4], [12], a principally different scheme of growth process was proposed (see Figure 1) which came to be known as Sublimation Sandwich Technique (SST). In this method the source of Ga vapor and the substrate were separated by a clearance of several millimeter forming a growth cell. This growth cell was placed into a temperature-gradient zone to initiate material transport from the source to the substrate. To provide a supply of reactive nitrogen into the growth cell, the cell was purged by ammonia flow. One of the advantages of this scheme was an ability to intensify mass transport in the growth cell due to decrease of the clearance between the source and the substrate. There-with not only high growth rates (up to 1 mm/h) were achieved but also complete (without losses) transfer of the source material to the substrate was attained [13]. Characterization of the GaN crystals grown by SST performed by different groups [14], [15], [16], [17], [18] had shown high quality of the material, comparable in

specific cases to that of GaN epilayers obtained by Metal-Organic Vapor Phase Epitaxy (MOVPE) or Molecular Beam Epitaxy (MBE). The advantages of this technique — high growth rate, use of the simplest source species, high yield of the growth components, high crystalline quality of growth material — were found to be potentially promising for development of commercial GaN bulk crystal growth technology. For that reason SST has become popular and is now being developed in various research centers [3], [19], [20].

In this paper we consider the current status of the Sublimation Sandwich Technique, the mechanisms of GaN growth, specific features of the growth process, and results of characterization of the grown crystals. Both experimental data and numerical modeling are used for analysis of the growth process. Problems to be solved in the nearest future are discussed as well.

## 2 Experiment

GaN crystals are grown in a tubular quartz reactor with radio-frequency heating (simplified scheme of the reactor is shown in Figure 1). The growth process is carried out in ammonia flow passing over and through the growth cell placed inside the reactor on a graphite susceptor. Both horizontal and vertical configuration of the reactor are used. The horizontal configuration provides a more effective supply of ammonia in the growth cell, the vertical one is more suitable for longer process duration. Before growth, the reactor is evacuated to a pressure of less than  $10^{-2}$  torr and then purged by ammonia for 10 min to remove residual gases (first of all, oxygen).

The growth cell consists of a Ga source and substrate, both forming a "sandwich" where transport of the main growth species (Ga and  $\text{NH}_3$ ) occurs. The growth cell is placed in a temperature-gradient zone, so that there appears a certain temperature difference  $\Delta T$  between the source and the substrate. This temperature difference serves as the driving force for Ga transport inside the growth cell and GaN crystallization on the substrate. Normally the distance  $d$  between the source and the substrate (clearance) is varied from 2 to 5 mm [3]. Temperatures of the source and substrate are controlled by W-Re thermocouples.

A mixture of liquid Ga and GaN powder is usually used as the source of gallium. The experiments show that use of pure Ga as the source provides maximum growth rates but results in poorer temporal and spatial stability of source operation. In turn, use of pure GaN powder leads to partial decomposition of the source material into the liquid (Ga) and vapor ( $\text{N}_2$ ) phases starting immediately after the beginning of the growth process. Again, in this case growth proceeds mainly from the mixture of liquid gallium and GaN.

Both sapphire and 6H-SiC(0001) Si and C faced are used as the substrates. SiC substrates are etched in KOH melt at the temperature of 480°C to remove a damaged surface layer arising from grinding and to determine the polarity of the substrate. Then SiC substrates are boiled in a diluted solution of acetic acid, and after that is rinsed in deionized water.

Growth of GaN crystals is carried out at atmospheric pressure in the temperature range of 1000-1300°C. The temperature difference between the substrate and the source is varied from 10°C to 100°C. The inlet ammonia flow rate of 150-850 sccm is maintained during the growth process. GaN crystals 70-800 μm thick are grown with deposition time being between 5 and 120 min. The typical size of the GaN crystals obtained is 0.5×15×15 mm. A number of crystals of size 25×25 mm are also grown with somewhat lower thickness. Growth rate is varied from 0.1 to 1.1 mm/h. The crystals of best crystalline quality are obtained with growth rates of 0.2-0.4 mm/h. A photo of a typical GaN crystal grown by SST is given in Figure 2. A dark area in the center of the crystal is proved to be attributed to Ga droplets accumulated at the interface between sapphire and the GaN layer. The appearance of the Ga droplets at the initial stage of growth is discussed in Section 4.4. The non-uniform distribution of droplet density over the sample is related to lowering of V/III ratio at the center of substrate (see the next section).

The grown GaN crystals are characterized by Hall measurements of carrier concentration and mobility, room-temperature photoluminescence, by the Color Cathodoluminescence Scanning Electron Microscopy technique, by differential double-crystal and triple-crystal X-ray diffractometry, and by electron paramagnetic resonance.

### 3 Modeling of GaN growth by Sublimation Sandwich Technique

To analyze in detail the gas-flow dynamics in the reactor and the concentration distribution of the main gaseous species we use a numerical simulation of the growth process. The mathematical model applied is based on the Navier-Stokes equation and includes the conservation equations for momentum, mass and energy as well as boundary conditions accounting for heterogeneous chemical reactions both on the surfaces of the source and the substrate. It is assumed that gas flow in the reactor is axisymmetrical. This allows us to perform two-dimensional modeling analysis of the growth process. Experimental data are employed to preset the temperature profile at the surface of quartz tube.

Transport of four gaseous species ( $\text{NH}_3$ ,  $\text{N}_2$ ,  $\text{H}_2$ , Ga) is considered without taking into account homogeneous chemical reactions between them (it is shown in

[21] that homogeneous cracking of ammonia is negligible up to temperatures as high as 1100°C). Based on the experimental data of Ref. [22] three-phase equilibrium (between solid GaN, liquid Ga and vapor phase) is assumed to be established at the surface of the source. Stoichiometric incorporation of gallium and nitrogen into the growing GaN crystal is also assumed.

We make one more assumption: that growth of GaN on the substrate occurs under mass transport limited conditions, i.e. that adsorption and desorption of gaseous species are the stages that limit the growth rate. In this case, surface processes can be described using the quasi-thermodynamic approach similar to that developed recently for analysis of MOVPE growth of group-III nitrides [23]. According to this approach, the kinetics of molecular nitrogen evaporation from the surface of GaN is accounted for by a temperature dependent sticking coefficient extracted from the experimental data on GaN free evaporation in vacuum [24]. The temperature independent sticking coefficient of ammonia is taken from Ref. [25].

Shown in Figure 3 is the geometry of the growth reactor of vertical configuration and the distribution of the ammonia concentration over the reactor (the temperature distribution and gas flow pattern in the reactor are given in Figure 4 and Figure 5 respectively). One can see that the  $\text{NH}_3$  concentration significantly decreases while gas flows from the inlet of the reactor (where pure ammonia is supplied) to the growth cell. Actually, the mole fraction of ammonia falls to  $5 \cdot 10^{-3}$ - $1 \cdot 10^{-2}$  inside the cell. The reason for this behavior becomes evident from Figure 6 where the 2D-distribution of concentrations of the main gaseous species (Ga,  $\text{NH}_3$  and  $\text{H}_2$ ) in the growth cell is plotted. A specific feature of the sublimation process is accumulation of molecular hydrogen inside the growth cell. Since homogeneous chemical reactions are not accounted for in the model, generation of  $\text{H}_2$  is related entirely to heterogeneous reactions proceeding on the surfaces of the substrate and the source. The mole fraction of  $\text{H}_2$  in the growth cell exceeds 93% so that it displaces the other species. This effect not only hinders the supply to the growth cell of ammonia but also favors the appearance of a lateral non-uniformity of V/III ratio and GaN growth rate. In the particular case plotted in Figure 3 and Figure 6, the concentration of Ga near the surface of the substrate increases by a factor of 1.3 from the center to periphery (the diameter of substrate is 30 mm) while the concentration of  $\text{NH}_3$  at the edge of substrate is approximately two times greater than that at the center. Correspondingly the  $\text{NH}_3/\text{Ga}$  ratio is equal to ~35 at the center of the substrate and to ~50 at the periphery. Therefore the results of modeling show that further optimization of the ammonia supply is

necessary in the vertical reactor to provide more uniform  $\text{NH}_3/\text{Ga}$  ratio distribution over the growth surface. In the horizontal reactor the  $\text{NH}_3/\text{Ga}$  ratio non-uniformity is related to depletion of the gas flow by the reactive species that can be diminished by substrate rotation.

The growth rate calculated for a substrate temperature of  $1150^\circ\text{C}$  and temperature difference  $\Delta T$  of  $50^\circ\text{C}$  is equal to  $\sim 0.1 \mu\text{m/h}$ . This value is 8-10 times less than the experimental value of the growth rate measured for these growth conditions. This remarkable discrepancy between the calculated and measured growth rates of the GaN crystal shows that traditional mechanisms of Ga transport (diffusion and convection) can not explain experimental observations. In more detail this question is discussed in the next section.

## 4 Mechanisms of GaN growth

In this section we discuss the mechanisms controlling the process of GaN growth by SST and factors limiting the growth rate. The nature of abnormally high Ga transport rate is considered as well.

### 4.1 Congruent and incongruent evaporation of the source material

First of all we discuss the difference in the growth process observed in our experiments and in the experiments of Ref. [26]. In [26] growth of GaN was carried out at lower temperature ( $\sim 1050^\circ\text{C}$ ). After 3 hours growth rate dropped drastically, and the growth process could not be restored with the same source material. Basing on mass spectrometry investigation of the source material the authors of [26] concluded that growth of GaN proceeded for the first 3 hours via transport of some volatile species such as  $\text{GaNH}$  or  $\text{GaN}_2\text{H}$ . Complete evaporation of these species from the source (apparently taking place after 3 hours of growth) resulted in the drop of the growth rate.

We think that transport of gallium observed in [26] during the first 3 hours occurred through a number of volatile species containing, along with the Ga and N atoms, oxygen and carbon. This assumption is supported by the fact that in the mass spectrum shown in Figure 8 of [26] the dominating species are N (14),  $\text{H}_2\text{O}$  (18),  $\text{N}_2$  or CO (28), Ar (40),  $\text{CO}_2$  or  $\text{N}_2\text{O}$  (44). The masses 84/85 and 96/98 attributed in [26] to  $\text{GaNH}$  and  $\text{GaN}_2\text{H}$  can be alternatively associated with  $\text{GaCH}_3$  or  $\text{GaO}$  and  $\text{GaCN}$  or  $\text{GaCO}$  respectively. The heaviest mass, 171, observed in the spectrum may be the  $\text{Ga}_2\text{O}_2$  radical. In addition to all these species, the contribution to growth of liquid gallium (69/70 masses in the mass spectrum) has to be taken into account as well (the micro-droplets of gallium could be trapped into the source material during the preparation procedure [21]). After these species are consumed, the gallium supply at the growth surface

can be provided by evaporation of the remained GaN powder. Apparently under conditions used in [26] the evaporation of GaN is congruent, and it is expected to be suppressed by the ammonia atmosphere in the reactor. In this case, the growth rate of GaN on the substrate should drop compared to that at the initial stage of the growth process.

In contrast, in our experiments (typical temperatures are  $\sim 1100\text{-}1250^\circ\text{C}$ ) the GaN powder in the source evaporates incongruently, i.e. with decomposition into the liquid and vapor phases. As a result, no deficit of the volatile species is observed — the growth process continues almost up to the moment of complete evaporation of the source material.

### 4.2 Transport of gallium between source and substrate

Comparison of theoretical and measured data shows that the experimental growth rate systematically exceeds the calculated values at least by a factor of ten. This implies that the mechanism of Ga transport is different from that accepted in our calculations. Another evidence of a specific mechanism of Ga transport is provided by Figure 7, where the dependence of GaN growth rate on the clearance  $d$  between the source and substrate is plotted. It is seen from Figure 7 that growth rate decreases more rapidly than  $1/d$  as one could expect assuming that diffusion is the prevailing mechanism of transport. These facts stimulated us to carry out a special investigation of the Ga transport in the sandwich system.

We measure the Ga transport rate in the sandwich system under various conditions:

- i) in argon atmosphere at a pressure of 1 atm (resistive heating of the susceptor),
- ii) in ammonia atmosphere at a pressure of 1 atm (radio-frequency heating of the susceptor), and
- iii) under low background pressure of  $\sim 10^{-6}$  atm (resistive heating of the susceptor).

In the first two cases the Ga transport between the source and the substrate is expected to occur via diffusion and convection, while in the latter case, it should be of free-molecular character. Results of this study are summarized in Figure 8.

It is seen in Figure 8 that all experimental points obtained are bordered by two calculated lines. One of the lines corresponds to pure diffusion of Ga from the source to the substrate. Another one describes free evaporation of Ga in vacuum (actually this curve represents a physical limit for the evaporation rate). Both lines have nearly an equal slope. In experiment the gallium flux measured in Ar atmosphere (under resistive heating of susceptor) corresponds exactly to the Ga transport by diffusion. At the same time experiments on free evaporation of Ga in vacuum and the measurements carried



out under the actual growth conditions ( $\text{NH}_3$  atmosphere) give nearly identical results which are less by the factor 30 than the calculated evaporation rate of Ga in vacuum.

To understand this abnormally high rate of Ga transport between the source and the substrate we consider three effects:

- i) gas convection in the growth cell enhanced by hydrogen generation at the surface of the source due to  $\text{NH}_3$  cracking,
- ii) multiple channel desorption of Ga (via gaseous compounds with hydrogen and other possible species), and
- iii) generation of Ga droplets at the surface of the source followed by their transport to the substrate.

Actually, the effect of convection is accounted for while modeling the growth process. but it does not provide the observed values of growth rate. To estimate the effect of multiple channel desorption we consider additional formation of GaH, GaH<sub>2</sub> and GaH<sub>3</sub> at the surface of the source as well as of the adduct Ga·NH<sub>3</sub>. As a result, the contribution of these species to Ga desorption from the source was found to be negligible. The role of other gaseous species (probably formed during preparation of the source material) is excluded by experiments carried out with pure liquid gallium. Therefore, the first two possible reasons for abnormally high rate of Ga transport cannot explain properly the experimental observations. Thus, the most probable origin of the high Ga transport rate is related to droplet generation. The nature of this effect is assumed to come from the liquid surface instability. In turn, the instability can be caused by different factors — axial temperature gradient in the growth cell directed opposite to the gravity force; lateral temperature gradient inducing Marangoni convection near the surface of the liquid; nucleation of GaN microcrystals near the walls of the growth cell resulting in a foam-like material formation [21], etc. At the moment there it is not possible to select the only reason for the instability so that the nature of the high gallium transport rate remains not completely understood.

### 4.3 Physical limitation of GaN growth rate in Sublimation Sandwich Technique

Of a special interest is the question of what maximum growth rate can be achieved using SST. To estimate the maximum achievable growth rate we develop a simplified model where transport of Ga considered as collisionless with the correction coefficient  $\alpha_{\text{Ga}}^{\text{trans}}=0.03$ , accounting for the difference between the Ga flux calculated for free evaporation in vacuum and the experimentally measured value. Another parameter of the model is the coefficient  $\alpha_{\text{NH}_3}^{\text{ise}}$  which accounts for the effective-

ness of the ammonia supply into the growth cell. Actually, this coefficient can be defined as the product of the ammonia sticking coefficient on GaN surface [25] and the ratio of  $\text{NH}_3$  partial pressure inside the growth cell to its partial pressure at the inlet of the reactor. Then, using the quasi-thermodynamic approach similar to that proposed in Refs. [23] and [24], we can calculate the growth rate of GaN in a sandwich system.

Figure 9 shows the temperature dependence of the growth rate calculated for  $\Delta T = 80^\circ\text{C}$ , ammonia partial pressure of 1 atm at the inlet of reactor, and different

values of  $\alpha_{\text{NH}_3}^{\text{ise}}$ . For comparison, experimental data are plotted in this figure corresponding to selected growth conditions. One can see that good agreement between the theory and experiment is achieved for  $\alpha_{\text{NH}_3}^{\text{ise}}=1\cdot 10^{-4}$ .

The value of  $\alpha_{\text{NH}_3}^{\text{ise}}$  estimated on the basis of 2D-calculations (see Section 3) for these growth conditions lies in the range of  $2\cdot 10^{-4} - 4\cdot 10^{-4}$ .

It was already mentioned in Section 3 that the supply to the growth cell of ammonia is far from optimal. Under ideal conditions all the ammonia arriving at the inlet of the reactor is transported to the substrate. In this case  $\alpha_{\text{NH}_3}^{\text{ise}}$  is equal to the  $\text{NH}_3$  sticking coefficient, i.e. 0.04 [25], and the estimated maximum achievable growth rate is equal to 15-20 mm/h.

### 4.4 Growth window for the Sublimation Sandwich Technique

The estimation of the GaN growth rate made above takes into account only limitations related to the rate of Ga transport to the growing surface. At the same time other factors can be important introducing additional limitations on the growth process. Among these factors are formation of liquid Ga on the growth surface, failure of epitaxial growth resulting in polycrystal formation, surface morphology degradation, etc. Obviously, the impact of these factors depends on the chosen growth conditions.

As was already mentioned, key parameters of the growth process are substrate temperature  $T$  and the temperature difference between the source and the substrate  $\Delta T$ . In addition, the flow rate of ammonia can be easily varied while keeping constant pressure in the reactor. Analyzing a large number of experimental data we can conclude that there exists some "growth window" in coordinates  $\Delta T - T$  where single GaN crystals can be obtained (see Figure 10). Beyond this window various factors interfere with growth. Indeed, the boundaries of the "growth window" are not definitely shaped, and they indicate some transition regions rather than a

sharp line corresponding to drastic change in the growth mode. That is why the diagram shown in Figure 10 has, first of all, a qualitative character.

One can see from Figure 10 that at high temperature and/or high  $\Delta T$  growth of GaN is interfered with by liquid droplets formation on the surface. This results in surface morphology degradation, the appearance of Ga inclusions in the crystal and a considerable rise in material defects. It is interesting that a forerunner of this process is the formation of liquid Ga inclusions at the interface between the substrate and the grown GaN crystal (such inclusions are absent in the bulk of the crystal). The photo of the GaN crystal shown in Figure 2 corresponds to just this situation. Ga droplets at the interface are found by inspection through transparent sapphire substrate in an optical microscope. The appearance of the liquid phase can be suppressed by increasing the  $\text{NH}_3$  concentration in the growth cell.

At low substrate temperature, epitaxial growth of GaN fails, and instead of a single crystal, polycrystalline material is observed to form.

At low  $\Delta T$  the gallium evaporation rate at the source becomes comparable to the gallium re-evaporation rate at the growing surface. In this case growth rate decreases that results in islanding of the grown material – the epitaxial layer becomes broken, and roughness of the surface gradually develops. If substrate temperature is increased, keeping  $\Delta T$  low, then liquid droplets start to form on the surface, and growth of GaN fails again.

A similar "growth window" can also be found for ammonia flow rate. At low flow rates there is a deficit of  $\text{NH}_3$  in the growth cell resulting in Ga droplet formation. An increase of the ammonia flow rate initiates growth of numerous needle crystals on the substrate. At the same time, inside the "window", growth of single GaN crystal takes place.

## 5 Initial stage of GaN growth

An interesting feature of SST is that no special buffer layer is required to grow GaN crystals of good quality. To study the initial stage of growth we apply the Color Cathodoluminescence Scanning Electron Microscopy (CCL-SEM) technique [27]. This method is based on visualization of luminescence locally excited by an electron beam at the cleaved plane of the grown crystal. It is believed also that the yellow emission band ( $\sim 2.5$  eV) in GaN is evidence of defective material. On the other hand luminescence of high-quality GaN lies in the ultraviolet (UV) spectral range, and therefore it is reproduced as a dark area in cathodoluminescence (CL) image. This difference in color allows us to reveal the areas of material with higher (yellow) and lower (dark area) defect density.

Figure 11 a shows a CL image micrograph of the cross-section of a GaN crystal grown directly on a sapphire substrate. It is seen that a defective layer ( $\sim 10$ - $15$   $\mu\text{m}$  thick) with yellow luminescence appears at the initial stage of growth. Then it gives a way to material of higher quality emitting in the UV spectral range (dark area in the micrograph). Notice the sharp change in material quality that is evident from the change of dominating emission wavelength. Further examination of the grown GaN crystal by the X-ray technique shows that near the boundary between the high-defect density and low-defect density layers, the density of threading dislocations decreases due to their bending.

Using a GaN buffer layer accelerates the formation of the good quality crystal. Figure 11b shows a CL image of a GaN crystal grown on a GaN layer ( $\sim 3$ - $5$   $\mu\text{m}$  thick) which was grown beforehand on a sapphire substrate by MOVPE. One can see from the figure that the GaN crystal formed by SST is less defective than the MOVPE buffer layer, which exhibits the yellow band emission.

We also compare the initial stages of GaN growth on sapphire and SiC substrates. Figure 11c shows the CL image of GaN grown on SiC(0001) Si-face surface. It is seen that no yellow luminescence is observed in the latter case even in the area adjacent to the substrate. Instead, blue emission located at the crystal-substrate interface is revealed by CCL-SEM. We can speculate that the possible origins of the blue luminescence are residual oxygen accumulated at the interface which then penetrates into the GaN crystal along microcracks, or elastic strain related to the twin and inversion domain boundaries.

Use of SiC(0001) C-face surfaces for growth of GaN does not give good results: the morphology of the GaN surface degrades very quickly. Such differences in the quality of GaN crystal grown on Si- and C-faced SiC surfaces can be understood from the fact that the face of SiC surface determines the polarity of the grown GaN crystal. According to Ref. [28], the formation of Si-N bonds on SiC(0001) Si-faced surface is thermodynamically favorable as well as formation of C-Ga bonds on SiC(0001) C-faced surface. Since GaN grows in 2D-mode via lateral spreading of the Ga-N bilayer, the initial Si-face of SiC surface provides a Ga-face surface of grown GaN crystal. It is well known that such a surface is smooth when growing GaN by any epitaxial techniques (MOVPE, MBE, HVPE) [29]. In contrast, an N-face GaN surface resulting from the initial C-face of SiC surface is rough and exhibits 3D pyramidal features. In this respect, growth of GaN on sapphire surfaces gives an intermediate result (more close to that obtained on SiC(0001) Si-faced surface) that is related to the mixed polarity of the grown GaN crystal.

## 6 Characterization of GaN crystals grown by the sublimation technique

### 6.1 X-ray characterization

Characterization of GaN crystals is carried out using double-crystal and triple-crystal X-ray diffractometry with  $\text{CuK}_{\alpha 1}$  and  $\text{MoK}_{\alpha 1}$  radiation. Both  $\omega$ - and  $\theta$ - $2\theta$ -scans are used for routine characterization of the material quality. To reveal in more detail the contribution of different factors to widening of the diffraction curves, measurements are carried out in different configurations (symmetric Laue-, symmetric and asymmetric Bragg-configurations) and for different reflections — (0002), (0004), (1010), (2020) and (1124).

The FWHM of the (0004)-reflection is systematically measured in  $\theta$ - $2\theta$ -mode on a large number of GaN crystals grown on sapphire and 6H-SiC(0001) Si-faced substrates. The FWHM of GaN grown on sapphire lies in the range of 6-9 arcmin while the FWHM of GaN crystals grown on a SiC substrate is between 2.5 and 6.5 arcmin. That GaN crystals grown on 6H-SiC have higher crystalline quality correlates with the data of CCL-SEM and morphology examination discussed in section 5.

Specific feature of the samples obtained by SST is their strong bending related to the difference in the lattice constants and thermal expansion coefficients of the substrate and the grown crystal. For example, radius of bending of 3  $\mu\text{m}$  thick GaN MOVPE layer grown on sapphire is  $\sim 23 \text{ m}$ . After further SST growth on this wafer, the 48  $\mu\text{m}$  thick GaN layer results in a bending radius of about 1 m (i.e. the crystal remains highly strained after cooling). Such a huge strain leads to break-down of the GaN crystals due to cracks during the growth process and especially after growth while cooling the sample. The cracks occur predominantly in the substrate in GaN grown on sapphire and in the epitaxial layer in GaN grown on 6H-SiC. Break-down of the samples due to cracks becomes an especially serious problem for crystals of increased thickness and lateral size.

Use of various scattering configurations and a number of diffraction reflections allows us to reveal the contribution of various factors to the FWHM of the diffraction curve. The three most important factors are considered — disorientation of the coherent scattering areas (blocks); size effect; and microdistortion of the crystalline lattice of material inside the blocks. It is found that the latter factor has a dominant contribution to the width of the diffraction curve. The size effect is also remarkable. At the same time the block disorientation has a minor effect on the width of the diffraction curve for GaN layers grown by SST.

We assume that the microdistortion of material inside the blocks is associated with dislocations of a dif-

ferent type. Extracting components of the microdistortion tensor from the X-ray measurements, we estimate the density of dislocations in the grown GaN crystals. Both screw and edge dislocation densities are found to be in the range of  $(1-2) \cdot 10^{10} \text{ cm}^{-2}$ . For comparison MOVPE GaN layers grown on sapphire have dislocation densities of  $\sim 6 \cdot 10^8 \text{ cm}^{-2}$  estimated in the same way. Of course, these estimates provide an upper limit for the dislocation densities in the crystals studied.

### 6.2 Photoluminescence and Hall measurements

A number of GaN crystals (25 samples) grown by SST were characterized by Hall measurements, Fourier transform spectroscopy and room-temperature photoluminescence (pumping of the samples was performed using a He-Cd laser with  $\lambda = 325 \text{ nm}$ ) in the spectral range of 0.5-3.5 eV.

All GaN samples studied exhibit n-type conductivity. Hall measurements and infrared ( $\lambda = 1-2 \mu\text{m}$ ) optical absorption give the value of electron concentration in the range of  $(2-6) \cdot 10^{17} \text{ cm}^{-3}$  and mobility between 30 and  $80 \text{ cm}^2/\text{V}\cdot\text{s}$ . Such low level of mobility is typical for unintentionally doped GaN crystals where the electron concentration is controlled by native defects.

A typical room-temperature emission spectrum of GaN grown on SiC(0001) under nearly optimal conditions is shown in Figure 12a. Here the intensity of the yellow emission band is at least ten times less than the intensity of the edge emission. The CCL-SEM study of the surface of the grown GaN shows that the yellow luminescence is located mainly near defects: microcracks, dislocations, twin and inversion domain boundaries (Figure 12 c), while far from defect areas no yellow emission is observed (Figure 12 b).

Deviation from the optimal growth conditions usually results in a considerable rise of the intensity of the yellow luminescence; it becomes comparable with that of the band edge. In addition, new long-wavelength emission bands appear. Figure 12d shows the CL image of the surface of GaN grown under non-optimal conditions. It is seen that a yellow-green emission dominates in CL spectra of such GaN crystals, and additional non-uniformity of the optical properties over the surface of GaN is observed.

### 6.3 Paramagnetic resonance study

The EPR spectra were studied using a conventional X-band (9.25 GHz) EPR spectrometer in the temperature range of 4-300 K. The study is carried out with GaN samples grown on 6H-SiC substrates.

Traces of Ni, Fe and Mn are found in some GaN crystals grown by SST. Most probably exist in the  $\text{Fe}^{3+}$ ,  $\text{Ni}^{3+}$  and  $\text{Mn}^{2+}$  charge states if these impurities occupy

Ga sites in GaN crystalline lattice. Impurity concentrations estimated based on the EPR measurements are  $10^{17}$ - $10^{18}$  cm<sup>-3</sup> for Fe, and  $10^{16}$ - $10^{17}$  cm<sup>-3</sup> for Mn and Ni. Fe and Mn contamination in GaN crystals may originate from the boat material of the Ga vapor source. Ni contamination may be attributed to the SiC substrate that was etched in molten KOH in a container made of Ni.

The energy level scheme of transition metals in GaN, as inferred from known levels in other III-V compounds via the Langer-Heinrich rule, indicates that the acceptor levels of Mn and Ni are close to mid-gap [30]. Therefore Mn and Ni seem to be more suitable impurities for fabrication of semi-insulating GaN substrates than previously discussed Fe and Cr.

New EPR lines associated with metastable defects are found in the GaN crystals. These lines exhibit a number of non-ordinary features. First, the EPR response has a strongly anisotropic g-factor. Second, a non-ordinary shape of the EPR lines, which looks like an absorption line, is observed. The next peculiarity is a strong temperature dependence of the EPR spectra. In Figure 13 typical EPR spectra recorded at different temperatures are shown. The g-factors for B||C increase considerably, while in the B⊥C orientation they decrease upon heating of the sample. Along with the changes in g-factors, a hysteresis in the temperature dependence of the line intensities is found. One can see in Figure 13 that at 50 K, the two new lines in EPR spectra disappear. Further cooling of the sample does not restore the line intensities. To recover the EPR signal the sample has to be heated up to the room temperature. The observed features are typical for defects with metastable configurations. Probably these defects can be related to the persistent photoconductivity discovered recently in GaN [31].

## 7 Conclusion

In this paper we discuss the current status of Sublimation Sandwich Technique with respect to growth of bulk GaN crystals. It is shown that SST allows high growth rate (up to 1 mm/h) and provides good quality for the grown GaN crystals. The crystalline quality of GaN depends on the substrate (the best results are obtained on 6H-SiC(0001) Si-faced surface) and the chosen growth conditions. High GaN growth rate observed in the experiment is assumed to originate from Ga droplets generation on the surface of the Ga source due to its instability. A "growth window" can be determined in SST for two main growth parameters — substrate temperature and the temperature difference between the source and the substrate.

As the experimental results and modeling show, SST growth of GaN crystals requires careful optimization of

the ammonia supply into the growth cell. At high process temperatures the NH<sub>3</sub>/Ga ratio in the growth cell not only influences the growth rate but also determines the defect density of the grown crystals. Further investigation of the mechanisms of Ga transport in the sandwich system are necessary for better stabilization of Ga source operation especially in growth processes of long duration.

The experiments also show that bending of GaN layers grown either on sapphire or on 6H-SiC substrates followed by cracking is a serious problem which hinders the increase of the thickness and lateral size of the crystals. The best way to overcome this problem is use of a homoepitaxial seed for further SST growth of GaN.

## REFERENCES

- [1] S Porowski, J Jun, P Perlin, I Grzegory, H Teissere, T Suski, *Inst. Phys. Conf. Ser.* **137**, 369-372 (1994).
- [2] A Usui, H Sunakawa, A Sakai, AA Yamaguchi, *Jpn. J. Appl. Phys.* **36**, L899 (1997).
- [3] Yu. A. Vodakov, E. N. Mokhov, A. D. Roenkov, M. E. Boiko, P. G. Baranov, *J. Cryst. Growth* **183**, 10 (1997).
- [4] Yu. A. Vodakov, M. I. Karklina, E. N. Mokhov, A. D. Roenkov, *Inorg. Mat.* **16**, 537 (1980).
- [5] CM Balkas, Z Sitar, T Zheleva, L Bergman, IK Shmagin, JF Muth, R Kolbas, R Nemanich, RF Davis, *Mater. Res. Soc. Symp. Proc.* **449**, 41-46 (1997).
- [6] G. A. Slack, T. F. McNelly, *J. Cryst. Growth* **34**, 263 (1976).
- [7] Z. A. Munir, A. W. Searcy, *J. Chem. Phys.* **42**, 4223 (1965).
- [8] R. B. Zetterstrom, *J. Mater. Sci.* **5**, 1102 (1970).
- [9] E. Ejder, *J. Cryst. Growth* **22**, 44 (1974).
- [10] T. Matsumoto, M. Aoki, *Jpn. J. Appl. Phys.* **13**, 1804 (1974).
- [11] D. Elwell, R. S. Feigelson, M. M. Simkins, W. A. Tiller, *J. Cryst. Growth* **66**, 45 (1984).
- [12] Yu.A. Vodakov, E.N. Mokhov, A.D. Roenkov, "Method of epitaxial growth of gallium nitride", Patent of USSR No 1136501 (1983)
- [13] E. N. Mokhov, Yu. A. Vodakov, *Inst. Phys. Conf. Ser.* **155**, 177 (1997).
- [14] C. Wetzel, D. Volm, B. K. Meyer, K. Pressel, S. Nilsson, E. N. Mokhov, P. G. Baranov, *Appl. Phys. Lett.* **65**, 1033-1035 (1994).
- [15] C Wetzel, D Volm, BK Meyer, K Pressel, S Nilsson, EN Mokhov, PG Baranov, *Mater. Res. Soc. Symp. Proc.* **339**, 453-8 (1994).
- [16] R. Heitz, P. Thurian, I. Loa, L. Eckey, A. Hoffmann, I. Broser, K. Pressel, B. K. Meyer, E. N. Mokhov, *Mater. Sci. Forum* **196/201**, 719 (1995).
- [17] L. Eckey, J.-Ch. Holst, P. Maxim, R. Heitz, A. Hoffmann, I. Broser, B. K. Meyer, C. Wetzel, E. N. Mokhov, P. G. Baranov, *Appl. Phys. Lett.* **68**, 415-417 (1996).
- [18] D. M. Hoffmann, D. Kovalev, G. Steude, D. Volm, B. K. Meyer, C. Xavier, T. Monteiro, E. Pereira, E. N. Mokhov,



- H. Amano, I. Akasaki, *Mater. Res. Soc. Symp. Proc.* **395**, 619 (1996).
- [19] S. Fischer, C. Wetzel, W.L. Hansen, E.D. Bourret-Courchesne, B.K. Meyer, E.E. Haller, *Appl. Phys. Lett.* **69**, 2716-2718 (1996).
- [20] S. Kurai, T. Abe, Y. Naoi, S. Sakai, *Jpn. J. Appl. Phys.* **35**, 1637 (1996).
- [21] S. S. Liu, D. A. Stevenson, *J. Electrochem.Soc.* **125**, 1161 (1978).
- [22] R. A. Logan, C. D. Thurmond, *J. Electrochem.Soc.* **119**, 1727 (1972).
- [23] S.Yu. Karpov, Yu.N. Makarov, V.G. Prokofjev, R.A. Talalaev, "Novel approach to simulation of group-III nitride growth by MOVPE", unpublished.
- [24] M. V. Averyanova, S. Yu. Karpov, Yu. N. Makarov, I. N. Przhevalskii, M. S. Ramm, R. A. Talalaev, *MRS Internet J. Nitride Semicond. Res. I*, 31 (1996).
- [25] M. Mesrine, N. Grandjean, J. Massies, *Appl. Phys. Lett.* **72**, 350 (1998).
- [26] S. Sakai, S. Kurai, K. Nishino, K. Wada, H. Sato, Y. Naoi, *Mater. Res. Soc. Symp. Proc.* **449**, 15 (1997).
- [27] G. V. Saporin, S. K. Obyden, M. V. Chukichev, S. I. Popov, *J.Lumin.* **31/32**, 684-686 (1984).
- [28] R. B. Capaz, H. Lim, J. D. Joannopoulos, *Phys. Rev. B* **51**, 17755-17757 (1995).
- [29] J. L. Rouviere, M. Arlery, R. Niebuhr, K. H. Bachem, Olivier Briot, *MRS Internet J. Nitride Semicond. Res. I*, 33 (1996).
- [30] J. Baur, M. Kunzer, K. Maier, et al., *Mater. Sci. Eng. B* **29**, 61-64 (1995).
- [31] C. H. Qiu, J. Y. Pankove, *Appl. Phys. Lett.* **70**, 1983 (1997).

FIGURES

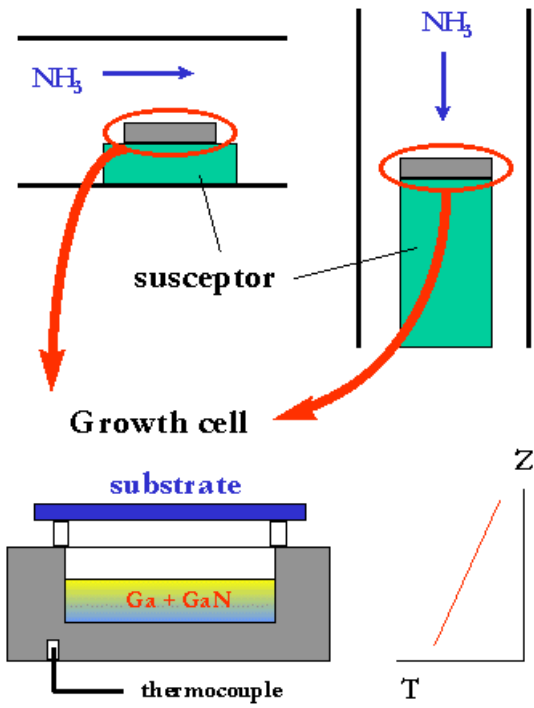


Figure 1. Simplified scheme of GaN growth by Sublimation Sandwich Technique.

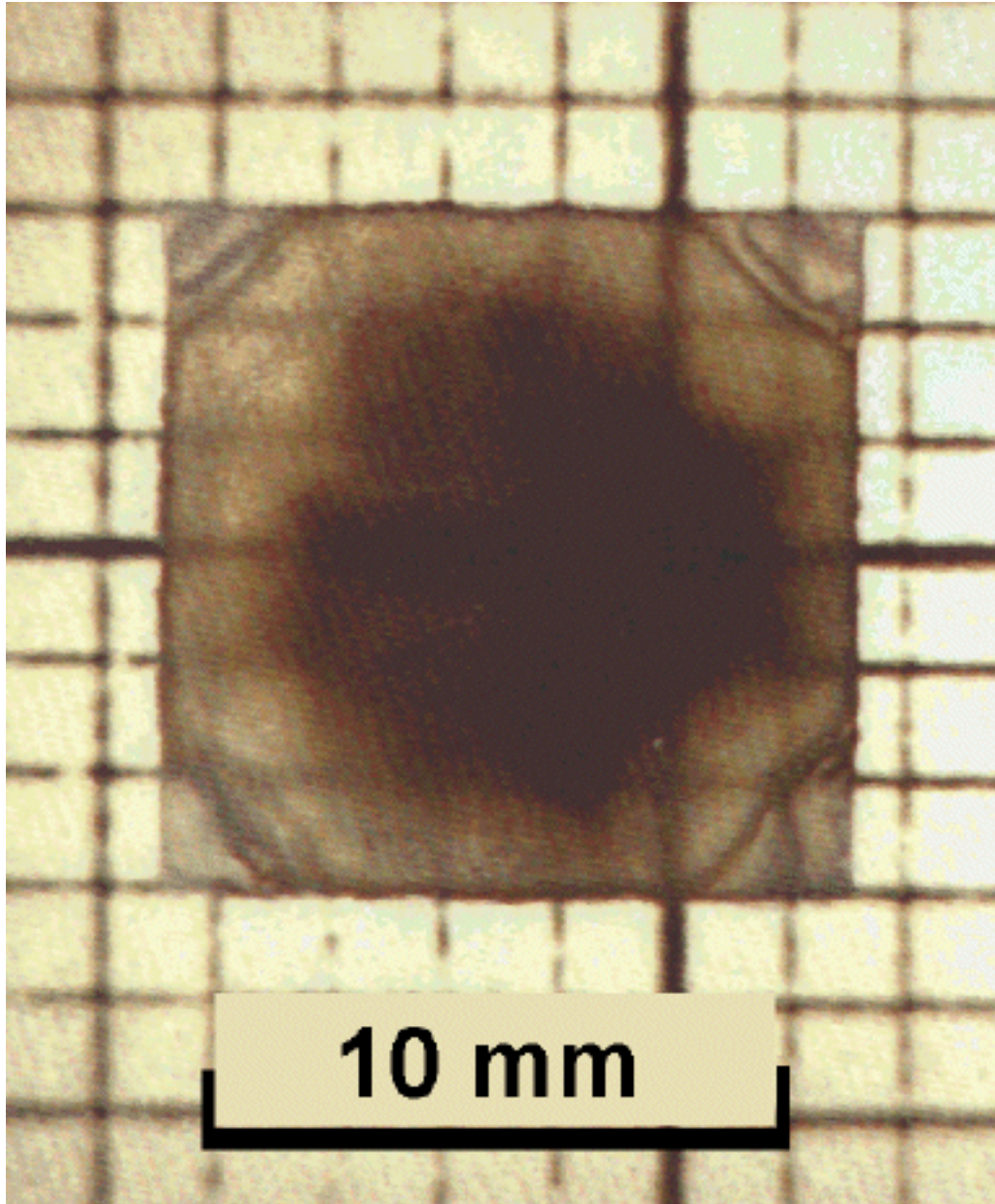


Figure 2. Photo of GaN crystal grown on a sapphire substrate by the sublimation technique. The thickness of the crystal is 0.3 mm. The dark area in the center of the crystal is attributed to Ga droplets accumulated at the interface between sapphire and GaN. The appearance of the droplets at the initial stage of growth is related to lowering of V/III ratio over the substrate from the periphery to the center.

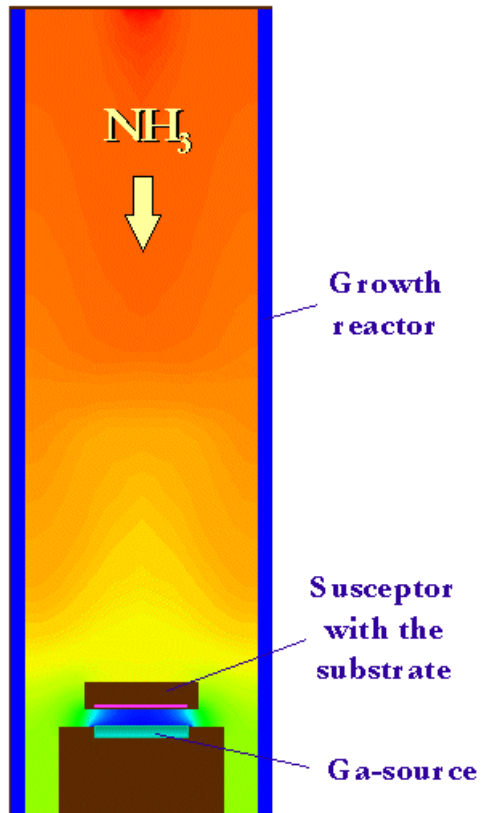


Figure 3. Distribution of ammonia concentration in the reactor of vertical configuration during sublimation growth of GaN. The color transition from blue to red indicates increasing ammonia mass fraction from 0.15 to 1.00. The substrate temperature is 1150°C, the temperature difference  $\Delta T = 50^\circ\text{C}$ .

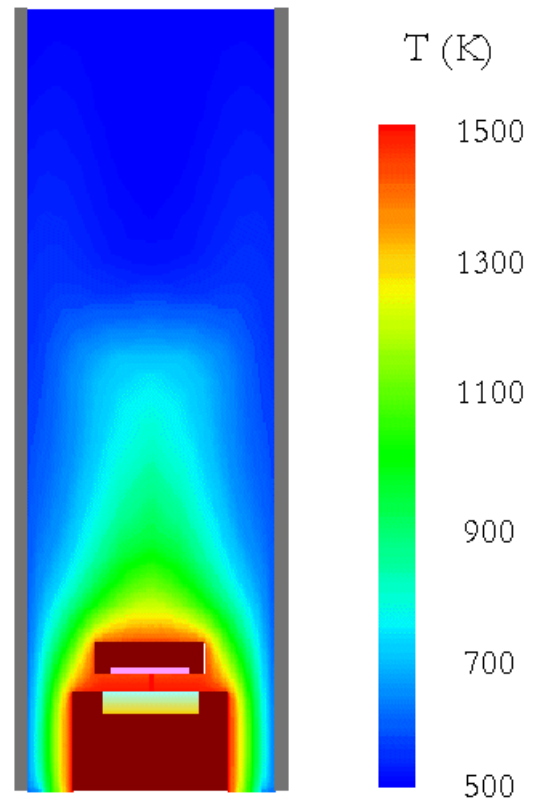


Figure 4. Typical temperature distribution in the reactor of vertical configuration during sublimation growth of GaN (the substrate temperature is 1150°C, and temperature difference  $\Delta T = 50^\circ\text{C}$ ).



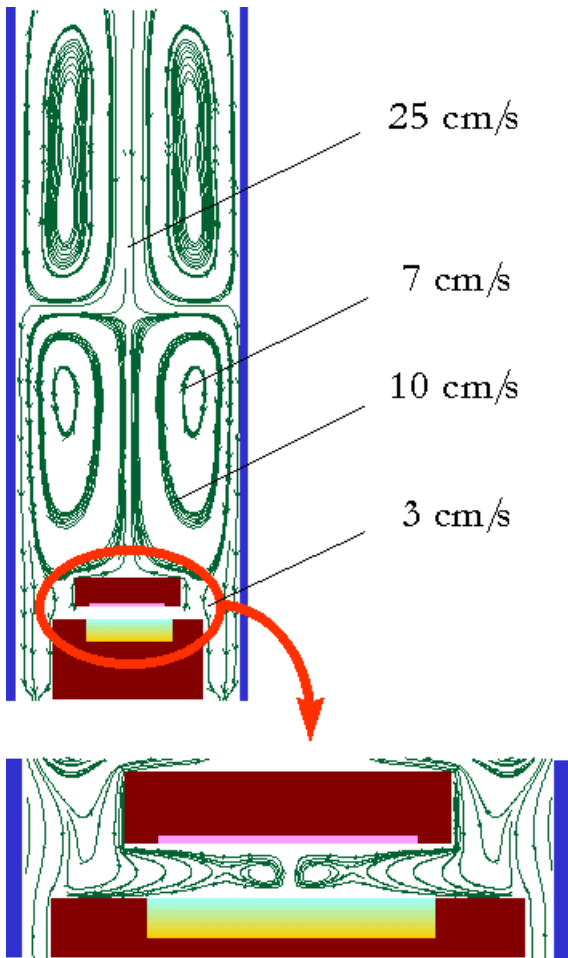


Figure 5. Streamlines of the gas flow in the reactor calculated for typical growth conditions (the substrate temperature is 1150°C, and the temperature difference  $\Delta T = 50^\circ\text{C}$ ).

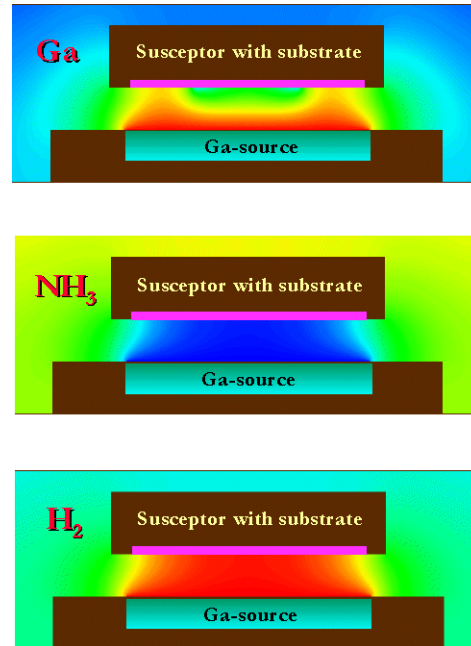


Figure 6. Concentration distributions of main gaseous species in the growth cell during sublimation growth of GaN. The color transition from blue to red indicates increasing species mass fraction (from  $8.6 \cdot 10^{-4}$  to  $7.9 \cdot 10^{-3}$  for gallium, from 0.15 to 0.73 for ammonia, and from 0.26 to 0.98 for hydrogen). The substrate temperature is 1150°C, the temperature difference  $\Delta T = 50^\circ\text{C}$ .

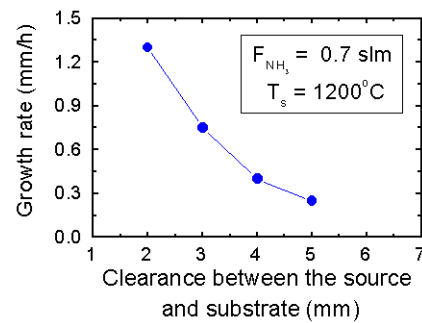


Figure 7. Growth rate versus clearance between the source and substrate measured for GaN crystals grown on sapphire.

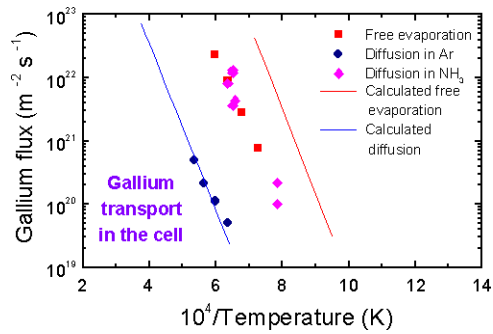


Figure 8. Gallium flux from the source to the substrate calculated for different evaporation modes and measured experimentally.

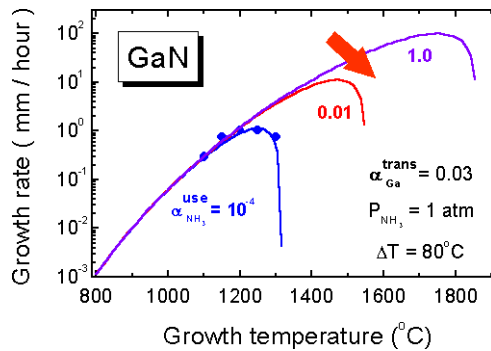


Figure 9. GaN growth rate versus temperature calculated for the sandwich system (solid lines). Blue circles are the experimental data obtained for these growth conditions. The red arrow indicates maximum growth rate achievable for the chosen  $\Delta T$  and reactor pressure, limited only by Ga transport.

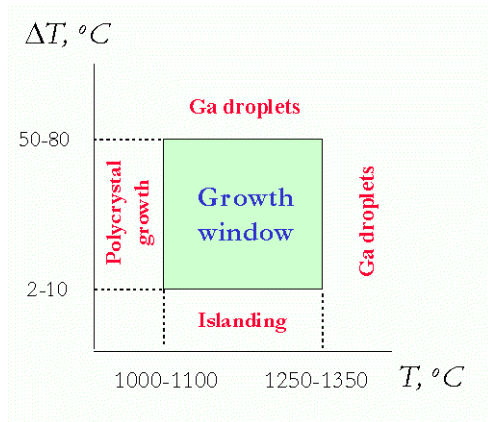


Figure 10. Schematic plot of the "growth window" related to Sublimation Sandwich Technique (reactor pressure is 1 atm).

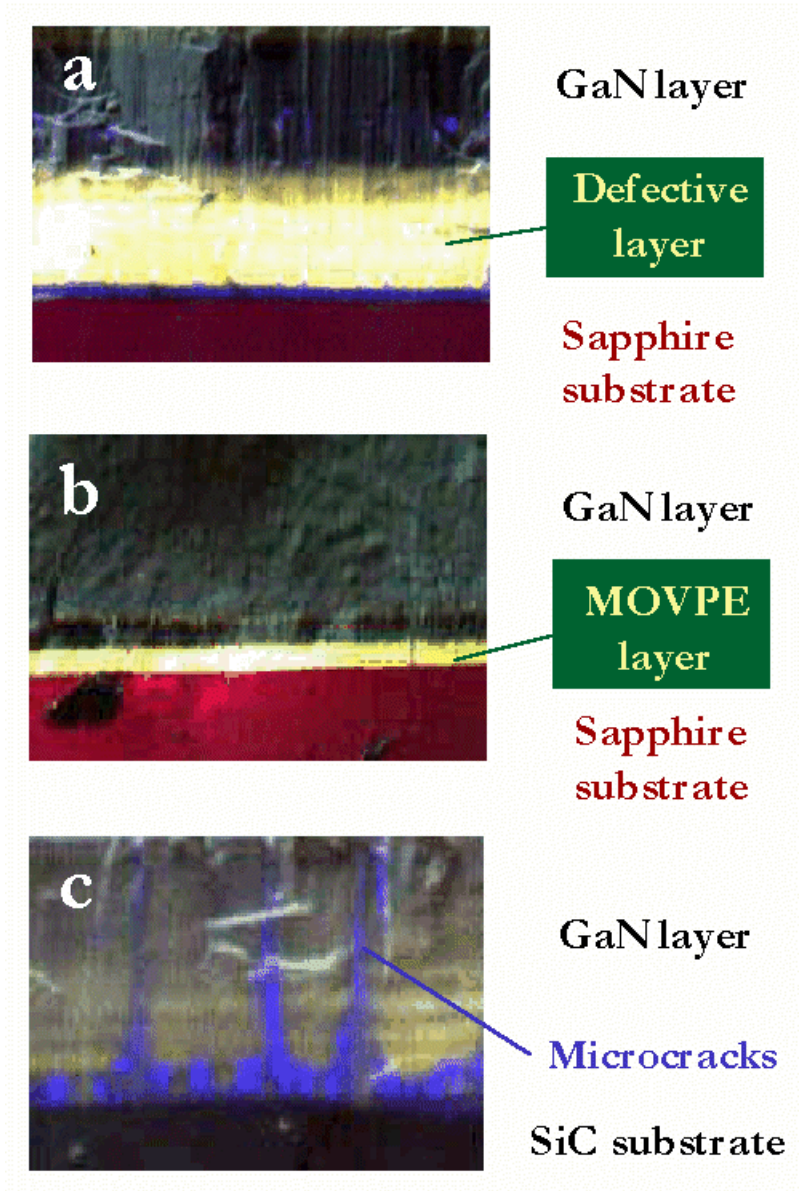


Figure 11. Color CL images of GaN crystals grown (a) directly on sapphire substrate, (b) on MOVPE layer (~5  $\mu\text{m}$  thick), and (c) on SiC(0001) Si-faced surface.

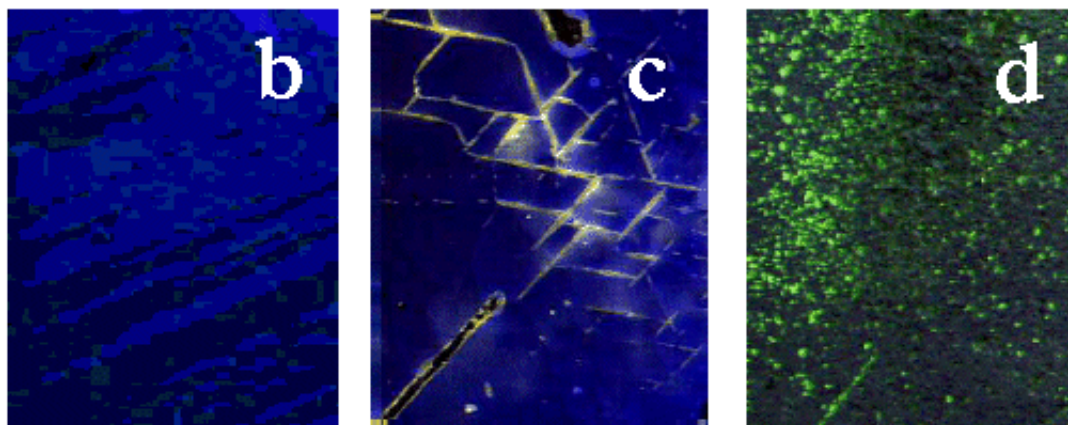
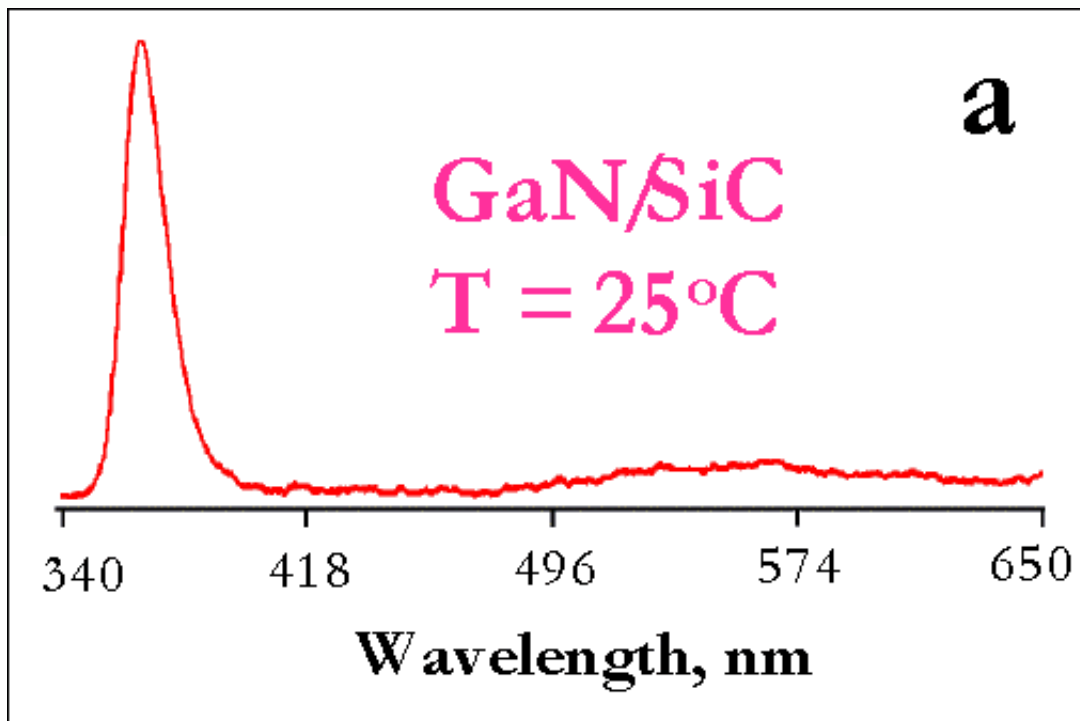


Figure 12. Photoluminescence and CCL-SEM characterization of GaN crystals grown by SST: (a) typical room-temperature emission spectrum of GaN grown on SiC(0001) Si-faced surface, (b) CL image of GaN surface far from defect area, (c) CL image of GaN surface near the defect area, (d) CL image of surface of GaN grown under non-optimal conditions.



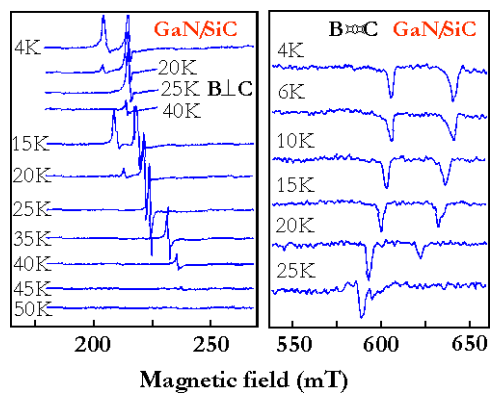


Figure 13. Temperature dependence of EPR spectra of GaN crystal grown on 6H-SiC(0001) Si-faced substrate. The spectra exhibit a hysteresis upon heating-cooling process that is an evidence of metastable defect formation.